Inorganic Chemistry

Article

pubs.acs.org/IC

Labile Zinc-Assisted Biological Phosphate Chemosensing and Related Molecular Logic Gating Interpretations

Kibong Kim, Yonghwang Ha, Léo Kaufman, and David G. Churchill*

Department of Chemistry, Korea Advanced Institute of Science and Technology (KAIST), 373-1 Guseong-dong, Yuseong-gu, Daejeon, 305-701, Republic of Korea

Supporting Information

ABSTRACT: Herein, molecular fluorescence 'OFF−ON' behavior with aqueous addition of biological phosphate and Zn^{2+} is studied with $Zn_2(slys)_2Cl_2$ [H_2slys = 6-amino-2-{(2-hydroxybenzylidene)amino}hexanoic acid], a fluorescent water-soluble complex, using various spectroscopic tools (e.g., ^{31}P NMR, UV−vis, emission, and CD spectroscopy) at the micromolar level. Adduct-dependent fluorescence intensity changes can be interpreted as a two-input (cation/anion) implication molecular logic gating system. A displacement study of PPi from the dizinc complex is also reported. Diphosphate and triphosphate addition/displacements were also studied. ^{31}P NMR spectroscopy shows gradual NMR peak shifts from bound ADP/GDP to free ADP/GDP with increasing [PPi]. In the emission spectrum, fluorescence quenching is shown: CD signal maxima decrease with addition of PPi. These displacement events are also tested with triphosphates (ATP, GTP), and their binding strength/displacement ability over ADP/GDP is quantified: PPi > ATP ≈ GTP ($3.35 \pm 0.77 \times 10^4$ M^{-1} for PPi, $7.73 \pm 1.79 \times 10^3$ M^{-1} for ATP, $9.21 \pm 2.88 \times 10^3$ M^{-1} for GTP over **1**·ADP). Many anions and cations were also screened for selectivity. Tubulin polymerization was assayed in the presence of **1** and its copper analogue which reflected a slight inhibition in polymerization.

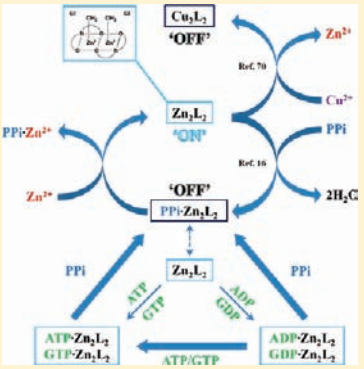

INTRODUCTION

Ions are generally important targets for chemosensors in biology. With respect to anions, phosphates are essential in biological processes.[1,2] In particular, nucleotide di/triphosphates such as ADP, ATP, GDP, and GTP are the main structural components of DNA and RNA. Further, ADP and GDP are the hydrolysis products of ATP and GTP, respectively. Pyrophosphate (PPi, $P_2O_7^{4-}$) is also a hydrolysis product of ATP.[3,4] Considering all of these closely related phosphates and their impact, synthetic molecular probes that can discern between such species are welcomed by the chemical and/or biological communities. Modes of detecting such important species by fluorescence and optical means via donor−acceptor recognition continue to be an active research aim. Receptor−analyte binding requires selective affinity and decent optical response changes as well as analytical sensitivity, etc. There are various reports about the detection of pyrophosphate and ATP.[5−15] Among them, zinc(II) complexes have been previously used for detection of PPi.[16−22] Also, there are some reports regarding displacement of phosphates with other phosphates from small molecule systems, but most of them relate to the indicator displacement assay-type approach which allows for colorimetric/fluorometric changes in detecting phosphate anions.[23,24] In brain mitochondria, phosphates can displace cytochrome *c* from the inner membrane by way of electrostatic interactions.[25] It is important and interesting to seek compounds that do not require independent detachable chromophores but instead rely on each other and on innate concentrations of phosphates directly. There are reports by Wittinghofer, Zhang, and co-workers about the displacement of GDP by GTP in the GTP-binding protein Ras which involves the catalytic action of guanine nucleotide exchange factors.[26,27] They studied displacement with fluorescence intensity changes aided by fluorescent-modified GDP/GTP. There are some phosphate displacement studies that involve the aid of metal ions. For instance, GDP displacement from tubulin by GTP in the absence of Mg^{2+} was studied.[28] In the adenosine unit case, ADP can be displaced by 1,N^6-ethenoadenosine triphosphate (ε-ATP) in the presence of Ca^{2+} on actin.[29] However, to the best of our knowledge, there is no work about phosphate−phosphate addition−displacement behavior studied directly by ^{31}P NMR spectroscopy.[30] In addition to anions, metal cations have innumerable roles and importance in biological processes in the human body and biology at large.[31−33] Metal ion homeostasis is also important and considered pertinent in varying degrees to the possible etiology of serious diseases such as Alzheimer's disease.[34,35] Among the ions, the zinc dication (Zn^{2+}) is important because its concentration in the human body affects and controls cellular systemic function, especially in neuronal systems.[36−38] Zn^{2+} is ubiquitous and essential. In health as well as in disease, the roles, transport, and concentration of Zn^{2+} are vital and therefore of significant research interest. Thus, detection of Zn^{2+} in water in vivo and

Received: September 6, 2011
Published: December 27, 2011

   dx.doi.org/10.1021/ic201948c | *Inorg. Chem.* 2012, 51, 928−938

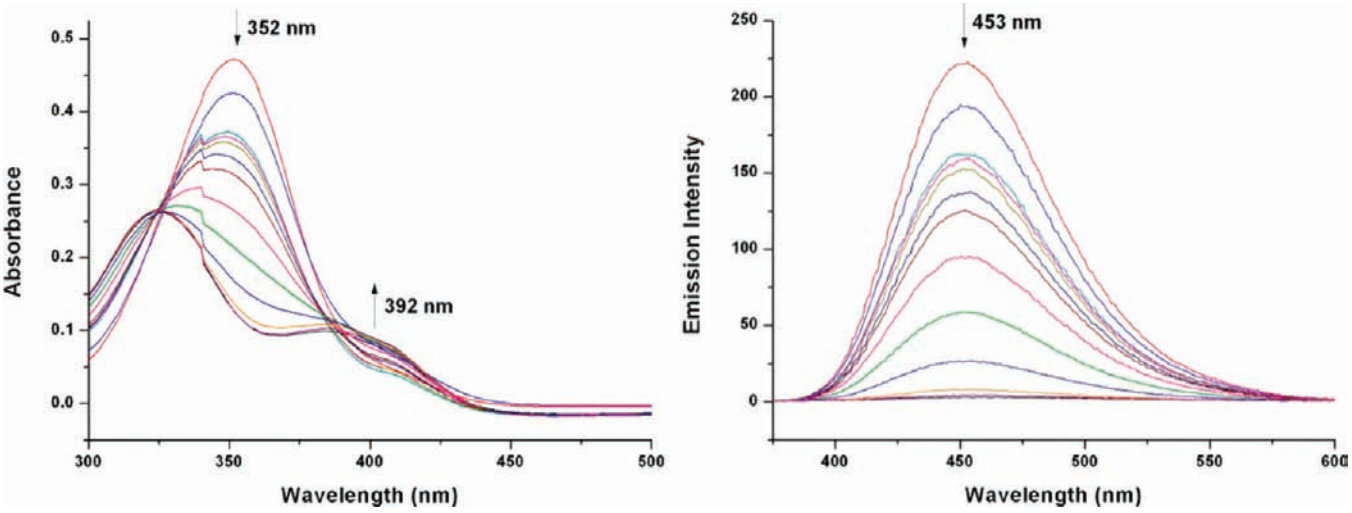

Figure 1. (Left) Absorption and (right) emission spectra (λ_{ex} = 352 nm) of **1**·ADP (50.0 μM) with titration of PPi (0−250 μM) in 10 mM HEPES buffer solution (H_2O, pH 7.4).

even in vitro remains a hot topic. However, despite all of the recent advances by major research groups such as that of Lippard and others, probe designs continue to require optimization for selectivity and sensitivity;[39,40] numerous results and conclusions about life are often based on and limited by colorimetric and fluorescent sensing techniques.[22,41−45]

On the basis of the type of (chemical) inputs and optical changes, certain logic gate operations (e.g., AND, OR, NOR, XOR, XNOR, INH, and IMP) can sometimes be usefully interpreted.[46−49] Fluorescence and absorbance changes are represented as the output signal and depend on the inputs which can be, e.g., chemical species, irradiation sources, and pH values. Thus far, there are many reports about AND and OR molecular logic gate systems,[50−54] but only a few implication (IMP) logic gate systems have been reported thus far.[55−60] To the best of our knowledge, there is no report about IMP molecular logic gating operated by anion tandem ligand exchange involving a metal cation input.

Tubulin is a ∼50 kDa protein and essential in the structure and support of the cell; it is recruited in cell division, cellular morphology, and transport and in the movement of the cell.[61] Tubulin can be classified into α- and β-tubulin, whose amino acid sequences are 40% identical. The α,β-tubulin heterodimer is a structural subunit of microtubulin. Each subunit has two guanine nucleotide binding sites.[62] Tubulin uses the dissociation energy of GTP at 37 °C to assemble tubules noncovalently. The subunits can rapidly associate and dissociate according to environmental responses.[63] There is much research about agents that activate or inhibit tubulin polymerization in cancer research.[64] In neurodegenerative research, tubulin is ubiquitous in neuronal cells. It is also supported by tau protein in brain neurons (axonal structure, etc.) and used for transporting various materials.[65] Under pathological conditions such as those of Alzheimer's disease the tau protein is adversely affected. It becomes hyperphosphorylated and separated from the microtubule and may self-aggregate into tangles. Loss of microtubule may induce neuronal cell death.[66,67] Thus, molecules that interact directly or indirectly with tubulin polymerization may be important in neurodegenerative probing or therapeutics.

Recently, our research group reported a fluorescent dizinc compound $Zn_2(slys)_2Cl_2$ (**1**) [H_2slys = 6-amino-2-{(2-hydroxybenzylidene)amino}hexanoic acid], which has the ability to selectively detect pyrophosphate through undergoing fluorescence quenching.[16] Previous studies have shown that this zinc complex has a binding tendency for various phosphate anions: ADP < ATP ≤ PPi. We wish to expand on this previous work and explore the possibility for biological phosphate *displacement* herein and Zn^{2+} sensing. Also, differences in tubulin polymerization behavior were tested with the dimetallic complex design and biological phosphate manifold.

EXPERIMENTAL SECTION

Materials and Synthesis. Sodium pyrophosphate, ADP (sodium salt), ATP (disodium salt), GDP (sodium salt), GTP (sodium salt hydrate), zinc(II) chloride, copper(II) chloride, HEPES, CHES, and MES were purchased from Sigma Aldrich Co. USA and used as received. Compound **1** ($Zn_2(slys)_2Cl_2$)[16] and **2** ([Cu-$(slys)_2$·$(H_2O)_2$]·$(ClO_4)_2$)[68] were synthesized by way of literature methods.

UV−Vis and Emission spectra. Absorption spectra were measured using a JASCO V-530 UV−vis spectrophotometer. Fluorescence measurements were performed with a Shimadzu RF-5301pc spectrofluorophotometer. A 0.01 M HEPES (pH 7.4) water solution was used as the solvent. For the displacement work, 1.0 equiv of the initial adduct was added to a solution of compound **1**. Then, the titrant is added in various amounts to the dizinc adduct solution (0.1, 0.2, 0.3, 0.5, 0.7, 1.0, 1.5, 2.0, 3.0, 4.0, and 5.0 equiv). To study Zn^{2+} sensing, 3.0 equiv of pyrophosphate was added to a solution of compound **1**. Then, Zn^{2+} was added in various amounts to the **1**·PPi solution (0.1, 0.2, 0.3, 0.5, 0.7, 1.0, 1.5, 2.0, 2.5, 3.0, 4.0, 5.0, and 7.0 equiv). Association constants were determined through the use of a literature method.[69] Solution CD spectra were carried out with a JASCO-815 CD spectropolarimeter in an aqueous HEPES buffer solution (10 mM, pH 7.4) using a cuvette of width 1.0 cm.

NMR Spectroscopy. ^{1}H NMR spectra were obtained in a D_2O solvent using a Bruker Avance 300.00 MHz spectrometer. A Bruker Avance 400 MHz spectrometer operating at 161.98 MHz was used for the ^{31}P NMR spectral measurements. The H_3PO_4 solution is used as an external standard for measurements. A H_2O (10 mM HEPES pH 7.4)/D_2O (85%/15%) solvent was used for Zn^{2+} sensing. For displacement studies, D_2O was used and NMR spectroscopic studies were performed in two ways. (i) Compound **1** and the first phosphate were mixed in a molar ratio of 1:1. Then, 5.0 equiv of the second phosphate was added and measured. (ii) Compound **1** and the first

dx.doi.org/10.1021/ic201948c | *Inorg. Chem.* 2012, 51, 928−938

phosphate were mixed in a 1:1 molar ratio. Then, the second phosphate was "titrated" where increasing amounts were present in the cuvette, i.e., 0.0, 0.2, 0.5, 1.0, 1.5, 2.0, 3.0, 4.0, and 5.0 equiv.

Tubulin Polymerization Assaying. The tubulin polymerization assay was performed with a commercial assay kit (Cytoskeleton Co., Cat. no. BK011P). A stock solution of tubulin protein and reagent were prepared according to product guidelines. Fluorescence intensity was checked through an HTS multilabel plate reader (PerkinElmer LAS model, Finland) at the Korea Research Institute of Bioscience and Biotechnology (KRIBB). The monitored excitation and emission wavelengths were 355 and 460 nm, respectively. Fluorescence intensity was checked every 1.00 min at 37 °C for 60+ min.

RESULTS AND DISCUSSIONS

Herein, a fluorescent dinuclear zinc compound was revisited. Compound **1**, $Zn_2(slys)_2Cl_2$ [H_2slys = 6-amino-2-{(2-hydroxybenzylidene)amino}hexanoic acid], was synthesized by a "one-pot" literature method.[16] It is water soluble, has blue fluorescence ($\lambda_{em,max}$ = 453 nm), and is compatible with biological systems. This complex previously showed binding properties with biological PPi and Cu^{2+}, resulting in fluorescence quenching.

Table 1. Conditional Binding Constants from Absorption and Emission Titration of Biological Phosphate Additions to the 1·ADP or 1·GDP Complex[69]

	absorption titration, M^{-1}	fluorescence titration, M^{-1}
titration of ADP to **1**	$3.17 \pm 0.21 \times 10^3$	$2.13 \pm 0.14 \times 10^3$
titration of GDP to **1**	$4.00 \pm 0.19 \times 10^3$	$3.00 \pm 0.20 \times 10^3$
titration of PPi to **1**·ADP	$3.35 \pm 0.77 \times 10^4$	$2.82 \pm 0.87 \times 10^4$
titration of ATP to **1**·ADP	$7.73 \pm 1.79 \times 10^3$	$9.57 \pm 2.93 \times 10^3$
titration of GTP to **1**·ADP	$9.21 \pm 2.88 \times 10^3$	$9.75 \pm 3.00 \times 10^3$
titration of PPi to **1**·GDP	$2.39 \pm 1.03 \times 10^4$	$3.41 \pm 1.45 \times 10^4$
titration of ATP to **1**·GDP	$1.14 \pm 0.41 \times 10^4$	$2.90 \pm 0.95 \times 10^4$
titration of GTP to **1**·GDP	$1.53 \pm 0.53 \times 10^4$	$1.95 \pm 0.88 \times 10^4$

Absorption and Emission Spectroscopy. The phosphate displacement phenomenon was studied by UV−vis absorption and fluorescence titrations (Figures 1 and S1−S12, Supporting Information). In the presence of 1.0 equiv of ADP with compound **1** in aqueous solution (pH 7.4, 10 mM HEPES H_2O buffer), PPi was titrated up to 5.0 equiv. In the absorption spectra, the peak at ~352 nm decreases, giving way to a new peak at 392 nm upon addition of PPi. This confirmed complete **1**·PPi complex formation.[16] Even though the anions are protonated at pH 7.4, conditional association constants (K_a at pH 7.4), based on UV−vis absorption titration data, were calculated (Table 1), $3.35 \pm 0.77 \times 10^4$ M^{-1} for the titration of PPi, $7.73 \pm 1.79 \times 10^3$ M^{-1} for the titration of ATP, and $9.21 \pm 2.88 \times 10^3$ M^{-1} for the titration of GTP, when using **1**·ADP as the target complex. These values are larger than those of titration of ADP and GDP to compound **1**, implying the possibility of displacement. Also, these values are smaller than those related previously reported constants through IDA and emission titration presumably because of the competing effects that exist with the dizinc-bound biological phosphate (i.e., ADP), a group more strongly binding than two chlorides or a colorimetric indicator group.[16] The binding stability order for compound **1** in the displacement situtation was confirmed to be PPi > ATP ≈ GTP. In the emission spectrum, the fluorescence signal ($\lambda_{em,max}$ = 453 nm) is quenched in the presence of 5.0 equiv of PPi. These results are coincident with formation of the

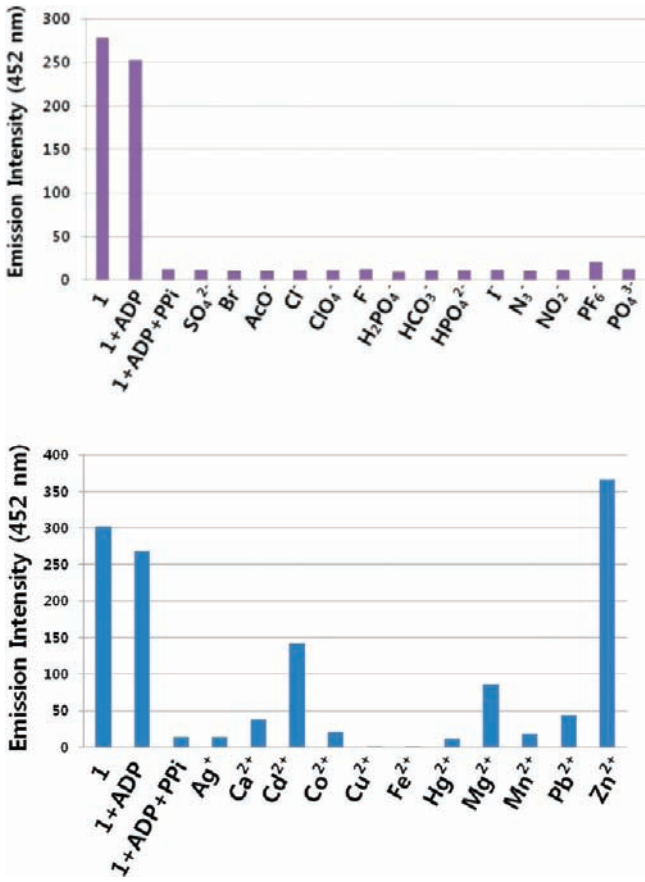

Figure 2. Emission intensity (λ_{ex} = 352 nm) of **1** (50 μM), **1** + ADP (50 μM), **1** + ADP + PPi (1:1:5; **1** = 50 μM), and **1** + ADP + PPi + anions/cations (1:1:5:10; **1** = 50 μM) in the presence of (top) other anions (sodium salt, 500 μM) or (bottom) other cations (perchlorate salt, 500 μM) in 10 mM HEPES buffer solution (H_2O, pH 7.4).

1·PPi complex; it is known that the presence of excess ADP does not effect fluorescence quenching.

ADP displacement by PPi is tested in the presence of excess amounts (10.0 equiv) of various representative and/or biologically relevant anions: Br^-, AcO^-, Cl^-, ClO_4^-, F^-, $H_2PO_4^-$, HCO_3^-, HPO_4^{2-}, I^-, N_3^-, NO_2^-, PF_6^-, PO_4^{3-}, and SO_4^{2-} (Figure 2, top, and S13−S15, Supporting Information). Even with the presence of excess anion, absorbance changes at 352 and 392 nm are almost perfectly retained. Also, fluorescence quenching at 452 nm was preserved in the presence of anions. Thus, in both cases these anions were found *not* to interfere in displacement of ADP by PPi. Also, various relevant metal cations were tested for competition or interference effects (Figure 2, bottom, and S16−S18, Supporting Information). Interestingly, Zn^{2+} reinstates the absorbance and fluorescence characteristics of compound **1**, suggesting that free Zn^{2+} binds to PPi and pulls it off from compound **1**. Loss of fluorescence with addition of Cu^{2+} and possibly Fe^{2+} can be seen. This might mean that these metals are displacing Zn^{2+} out of the complex. Mercury does not appear to perturb the system.

Through metal ion screening of compound **1** and bound PPi it was found that only free Zn^{2+} addition gives a sign of reversibility. Therefore, we expanded this work here as a concept of reversibility; recovery of blue fluorescence of **1** by removal of its PPi group with free metal ion and relating interactions and optical responses are presented and discussed

dx.doi.org/10.1021/ic201948c | *Inorg. Chem.* 2012, 51, 928−938

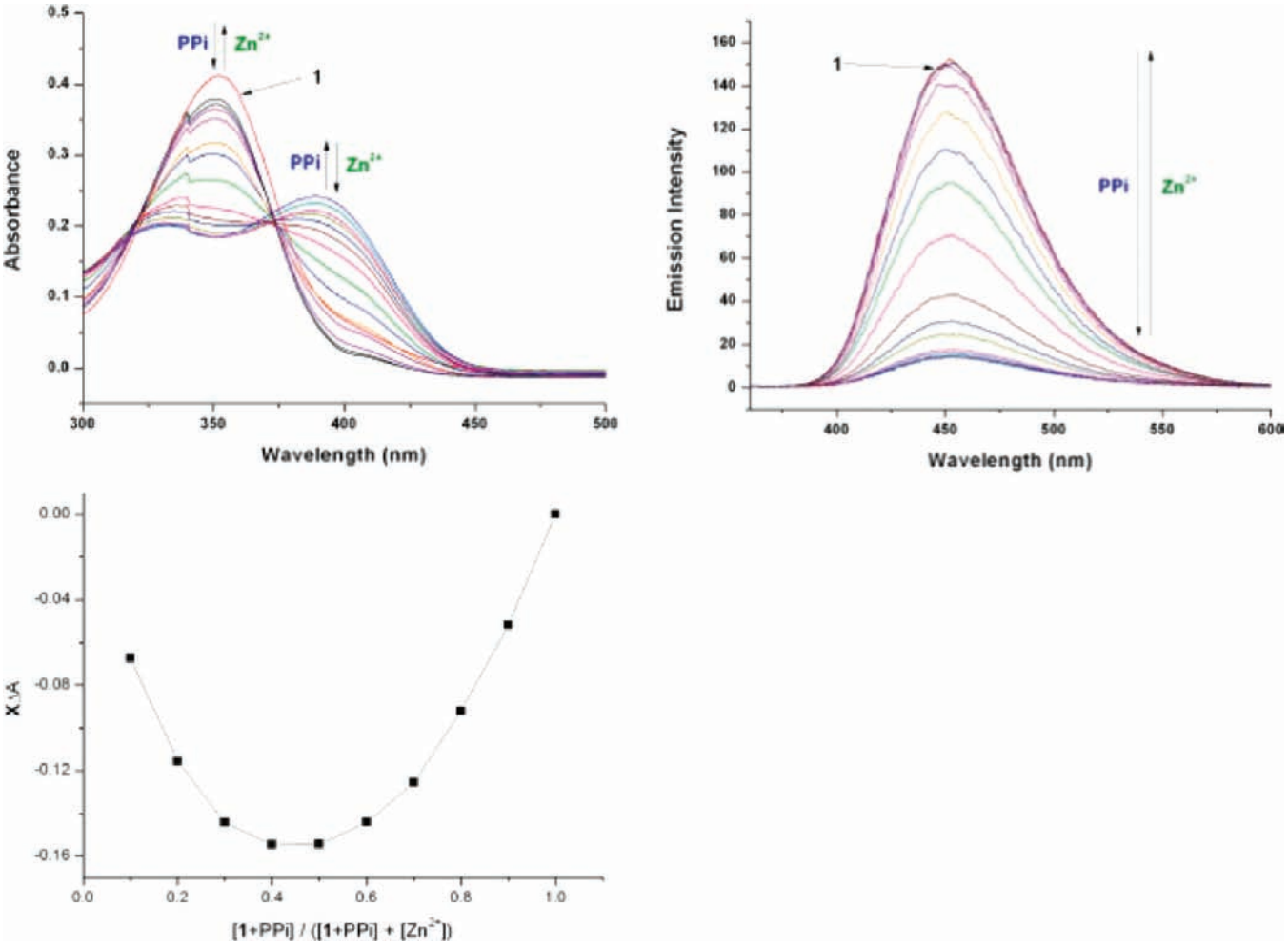

Figure 3. (Top left) Absorption and (top right) emission spectra (λ_{ex} = 352 nm) of the Zn^{2+} titration ($ZnCl_2$, 0.10−7.0 equiv) to **1** PPi (50:150 μM mixture). (Bottom) Job plot between [**1** + PPi] and [Zn^{2+}]. All measurements were performed in 10 mM HEPES buffer solution (H_2O, pH 7.4).

Table 2. Implication (IMP) Logic Gate System of Compound 1[a]

input 1, Zn^{2+}	input 2, PPi	output 1, fluorescence "ON" at 453 nm	output 2, absorbance at 392 nm
0	0	1	0
0	1	0	1
1	0	1	0
1	1	1	0

[a]Compound **1** (50 μM), PPi (3.0 equiv), Zn^{2+} (3.0 equiv) addition.

herein. Zn^{2+} titration of the **1**·PPi complex shows reinstatement of absorbance and fluorescence intensity (Figure 3). In the absorption spectrum, addition of PPi shows a new peak at 392 nm; a diminution of the $\lambda_{abs,max}$ band for compound **1** occurs at 352 nm. After addition of 3.0 equiv of PPi to **1**, Zn^{2+} is titrated to the mixture. With increasing amounts of [Zn^{2+}], the peak at 392 nm is diminished and a peak at 352 nm increases. After addition of 7.0 equiv of Zn^{2+}, the absorption spectrum of the final mixture is almost the same as that for compound **1**. Free Zn^{2+} and PPi do not give any absorption signal themselves. In the emission titration, PPi addition shows fluorescence

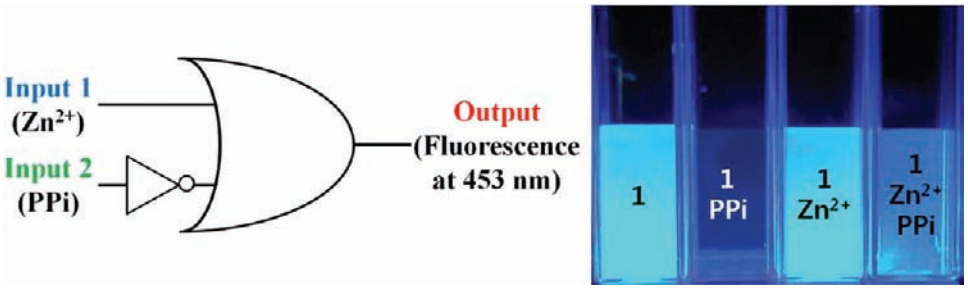

Figure 4. (Left) Diagram of IMP molecular logic gating adopted by this work. (Right) Photographs of a combination of compound **1**, PPi, and Zn^{2+} in 10 mM HEPES buffer solution (H_2O, pH 7.4) under UV light (365 nm).

dx.doi.org/10.1021/ic201948c | Inorg. Chem. 2012, 51, 928−938

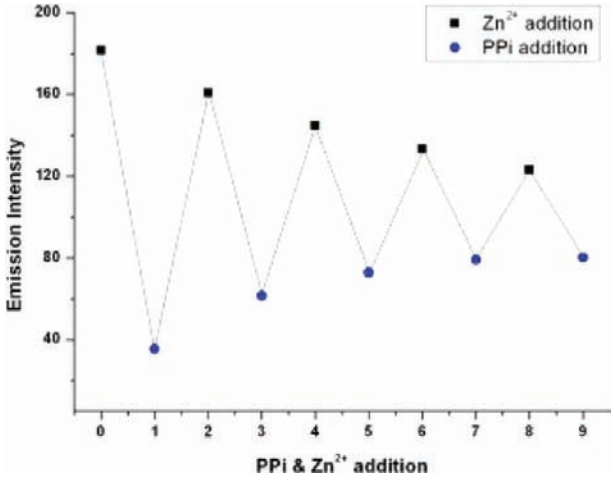

Figure 5. Emission intensity change (λ_{em} = 453 nm, λ_{ex} = 352 nm) of stepwise and alternate 3.0 equiv additions of Zn^{2+} (black squares) and PPi (blue circles) showing the reversibility of compound **1** (50 μM) in 10 mM HEPES buffer solution (H_2O, pH 7.4). Equilibration time = 1 min.

Table 3. Percentage of Emission Intensity Recovery and Conditional Association Constants Based on Different Phosphates

phosphate	% recovery[a]	association constants[b] ($K_a \times 10^4$ M^{-1})
PPi	20.5	0.848 ± 0.27
ADP	55.4	1.16 ± 0.19
ATP	35.0	2.11 ± 0.29
GDP	28.1	0.824 ± 0.16
GTP	42.4	2.38 ± 0.38

[a]Percentage of recovery (%) = {[F.I. (**1** + phosphate +1.0 equiv of Zn^{2+}) − F.I. (**1** + phosphate)]/[F. I. (**1**) − F. I. (**1** + phosphate)]} × 100). [b]Association constants are calculated from the emission titration of Zn^{2+} to **1** phosphate complexes.

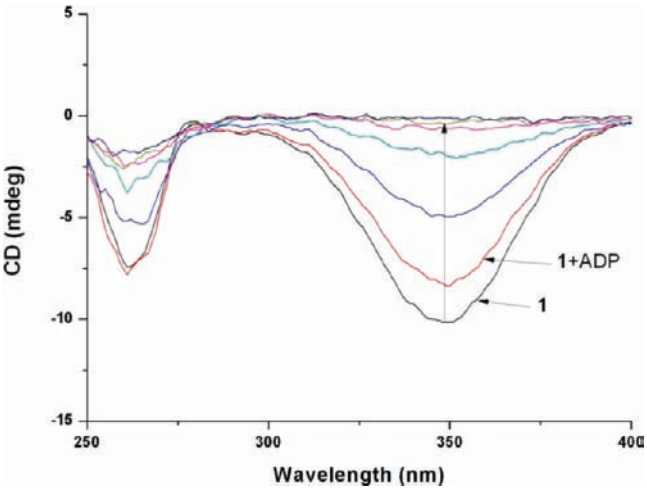

Figure 6. CD spectrum of **1**·ADP (50 μM) with titration of PPi (0–250 μM). Cell path length = 1.00 cm. All measurements were performed in 10 mM HEPES buffer solution (H_2O, pH 7.4).

quenching;[16] subsequent Zn^{2+} titration gives the return of emission intensity at 453 nm. After addition of more than 5.0 equiv of Zn^{2+}, the emission intensity is saturated around that expected for compound **1** alone. A Job plot study shows that incoming Zn^{2+} and the released PPi substrate are consistent with a 1:1 binding stoichiometry (Figure 3, bottom). Also, binding is tested with a range of pH values: 6.5, 7.0, 7.4, 8.0, 8.9, and 9.6 (Figures S19–S23, Supporting Information). Under neutral conditions (pH 7.0–8.0), absorbance changes and fluorescence 'ON' recovery behavior are more complete than at other pH values. Under basic conditions (pH 8.9 and 9.6), fluorescence recovery is not full, even at excess amounts of Zn^{2+} (7.0 equiv), implying strong binding between compound **1** and PPi in basic media.

On the basis of the fluorescence 'ON' and 'OFF' phenomena at 453 nm, IMP molecular logic gating behavior can be established (Table 2 and Figure 4). Two chemical species, Zn^{2+} and PPi, act as two inputs. Addition of free Zn^{2+} to compound **1** gives fluorescence 'ON' (1) signaling. However, fluorescence quenching is effective with addition of PPi (OFF, 0). Addition of PPi first followed by Zn^{2+} second results in fluorescence 'ON' (1) behavior. The photograph of these four solutions under UV light is shown in Figure 4 (λ_{exc} = 365 nm). Additionally, absorbance changes at 392 nm also can be interpreted as inhibition (INH) logic gating, the opposite result of IMP logic gating.

Next, the binding reversibility behavior between PPi and Zn^{2+} is tested (Figure 5). Addition of PPi gives a fluorescence decrease; Zn^{2+} addition gives an increase. These alternate additions (3.0 equiv each) are repeated. After 4.5 cycles, fluorescence 'ON' and 'OFF' behaviors are still clearly observed, even though emission intensity changes are smaller than those found initially. The possibility of aqueous dissociation of **1** into PPi-bound monomers with dimer restoration occurring upon excess free Zn^{2+} is a scenario not clearly supported by the current body of experimental evidence, but it cannot be ruled out either.

The success of the Zn^{2+}/PPi pair led us to expand to different and more complex biological phosphates such as ADP, GDP, ATP, and GTP. The phosphates added to compound **1** reduce fluorescence intensities to different degrees; addition of 1.0 equiv of Zn^{2+} leads to different "turn-ON" recovery ratios (Figures S24–S28, Supporting Information). In Table 3, percentages of emission intensity recovery are shown. Addition of 1.0 equiv of Zn^{2+} to **1**·PPi (Figure 3) has only 20.5% recovery, suggesting that there is stronger binding between **1** and PPi than with **1** and other biological phosphates. Association constants calculated from the fluorescence titration results also show smaller values for the **1**·PPi case over those for the other phosphates, except in the case of GDP. PPi uptake was also tested for free Cu^{2+}, in place of Zn^{2+} (Figure S29, Supporting Information). Titration of **1**·PPi (3.0 equiv) with Cu^{2+} ($CuCl_2$) gives further emission intensity decreases at 453 nm. After addition of 2.0 equiv of Cu^{2+}, complete fluorescence quenching is effected. In a previous report, addition of Cu^{2+} to a related dizinc system, $[Zn_2(sys)_2(NO_3)_2]$, results in direct displacement of two core Zn^{2+} ions by two Cu^{2+} ions, forming the related nonfluorescent dicopper complex.[70] We will return to a discussion of this species in the tubulin protein assay section below. The present titration result corresponds to two zinc centers at compound **1** being displaced by copper atoms and PPi being retained. From the results of the Cu^{2+} titration, NOR logic gating is interpreted by the two inputs, Cu^{2+} and PPi (Table S1, Supporting Information).

CD Spectroscopy. CD spectra were acquired and revealed the binding tendency of compound **1** which has a negative Cotton effect at 352 nm (Figure 6). Addition of 1.0 equiv of ADP gives a slight decrease in the CD spectral band. Further

dx.doi.org/10.1021/ic201948c | Inorg. Chem. 2012, 51, 928–938

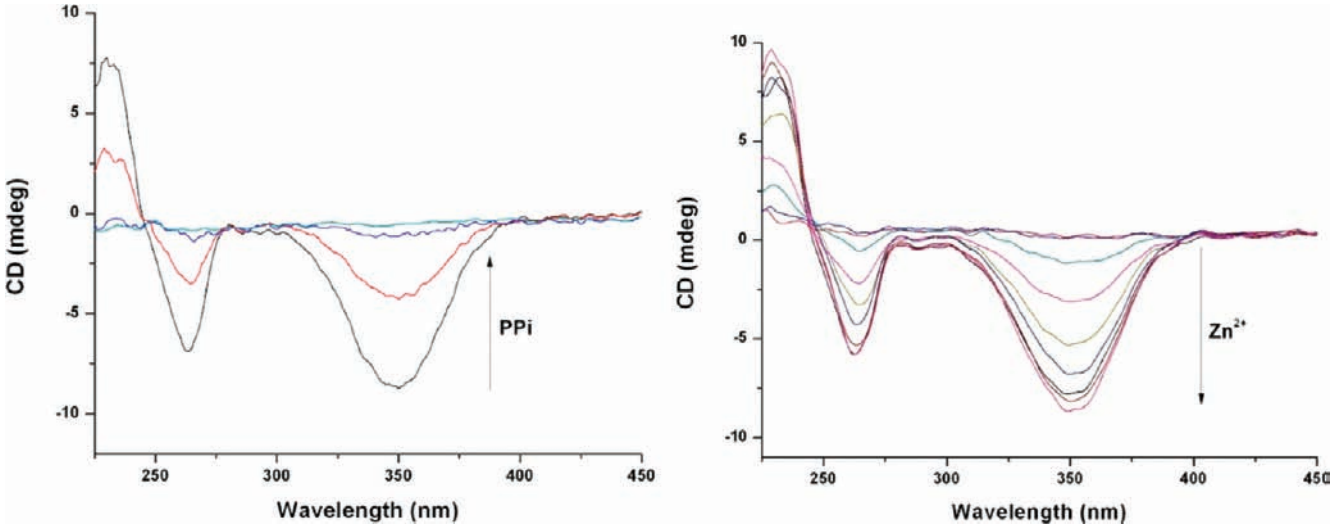

Figure 7. CD spectrum of (left) PPi titration (0.0−3.0 equiv) with **1** (50 μM) and (right) Zn^{2+} titration ($ZnCl_2$, 0.0−7.0 equiv) with **1** (50 μM)·PPi (150 μM). Cell path length = 1.00 cm. All measurements were performed in 10 mM HEPES buffer solution (H_2O, pH 7.4).

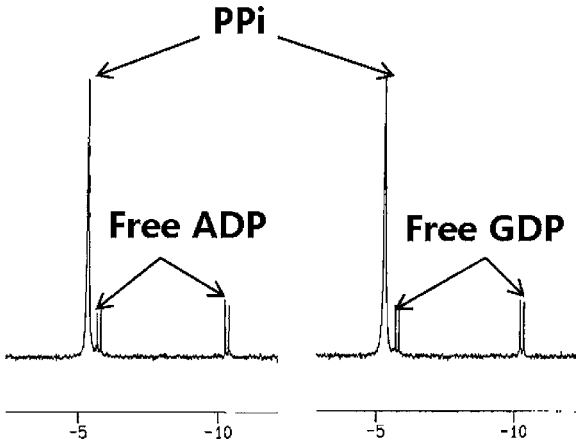

Figure 8. ^{31}P NMR spectra of (left) **1**·ADP (1.0 equiv) + PPi (5.0 equiv) and (right) **1**·GDP (1.0 equiv) + PPi (5.0 equiv) in D_2O.

addition of PPi gives a spectral decrease; finally, no chirality exists after addition of 5.0 equiv of PPi. Even with excess ADP, the CD signal does not completely disappear.[16] A loss of the Cotton effect with 5.0 equiv of PPi strongly supports the notion that bound ADP has been completely displaced by PPi. The CD spectral data also supports bound PPi uptake by Zn^{2+} (Figure 7). With addition of 3.0 equiv of PPi, a loss of the Cotton effect is monitored. Then following titration with Zn^{2+} a negative Cotton effect is stepwise restored, finally giving a signal similar to that of **1** (after addition of 7.0 equiv Zn^{2+}).

NMR Spectroscopy. ADP/GDP displacement by PPi was monitored through ^{31}P NMR spectra in D_2O (Figure 8 and Table 4). Addition of 1.0 equiv of ADP to **1** (0.01 M) shows **1**·ADP binding as judged by the appearance of new peaks at δ −6.23 and −9.22. Then addition of excess PPi (5.0 equiv) gave the disappearance of the peaks arising from formation of **1**·ADP; concomitant peaks at δ −5.75 and −10.30 are assigned to free ADP. Likewise, for GDP binding, **1**·GDP complexation gave spectral peaks at δ −6.17 and −9.31. After addition of 1 equiv PPi, a new peak at δ −4.51 appeared, assignable to the dizinc-bound PPi. Also, free GDP peaks were present (δ −5.74 and −10.28). Thus, we can strongly support displacement of ADP/GDP by PPi.

To facilitate a detailed study, ^{31}P NMR spectral *titrations* were also performed (Table 5, Figures 9 and S31−S36, Supporting Information). Chemical shifts from these titrimetric addition results are summarized in the Supporting Information. Figure 9 (top) shows ^{31}P NMR spectral changes of **1**·ADP upon titration with PPi in D_2O. With increasing amounts of PPi, ^{31}P nuclei of ADP were tracked moving from δ −6.23 and −9.22 (0 equiv of PPi) to δ −5.69 and −10.26 (5.0 equiv of PPi). Changes in chemical shifts correspond, albeit on the room temperature NMR time scale, to the bound ADP becoming free ADP. At low equivalency of PPi (<1.0 equiv) the chemical shift of PPi represents the zinc-bound analyte. However, with increasing amounts of PPi, the chemical shift moves upfield to δ −5.28 in the presence of 5.0 equiv of PPi. This chemical shift is quite close to that of free not bound PPi. To address whether the simple PPi δ peak shift was not a result simply of changes in [PPi], dilution studies were performed with ^{31}P NMR. At different concentrations, peaks of ADP and ATP alone have almost no shift (within 0.1 ppm). In the PPi case, with increasing concentration, peaks shift in the downfield direction: −6.16 (0.01 M) to −5.70 (0.05 M). Importantly, the shift direction of PPi alone upon increasing concentration is opposite to that for the PPi titration with **1**·ADP. Theoretically, two sets of peaks are expected: one set for bound and one for free PPi (two sets are found for bound and free ADP). Also, titration of ATP with **1**·ADP is performed in the same way (Figure 9, bottom). With increasing amounts of ATP up to 5.0 equiv, large NMR peak shifts occurred for two of the three peaks ($\Delta\delta$ 3.29 ppm for P_γ and $\Delta\delta$ 2.28 ppm for P_β). This pattern is interpreted as the P_β−O and P_γ−O groups binding to neighboring zinc centers, while the P_α−O group does not bind (only $\Delta\delta$ 0.21 ppm change). ADP peaks shift from δ −5.94 and −9.10 to δ −9.90 and −10.64, respectively. One apparent discrepancy we found is that the chemical shifts of free ADP after addition of 5.0 equiv of PPi and ATP are different: δ −5.69 and −10.26 for the PPi titration and δ −9.90 and δ −10.64 for the ATP titration. One possible reason is that the presence of Na^+ is able to affect chemical shift behavior. In the literature, two different sets of ^{31}P NMR spectroscopic peaks for free ADP are found; one report[16] shows the former case, and the other report shows the latter set of values.[71] The

dx.doi.org/10.1021/ic201948c | *Inorg. Chem.* 2012, 51, 928−938

Table 4. Resulting ^{31}P NMR Spectroscopic Resonances after Addition of 5.0 Equiv of Titrant to 1 and Bound Phosphates in D_2O Solvent

		titrant (5.0 equiv)					
		PPi	ADP	ATP	GDP	GTP	HPO_4^{2-} (2.98)
bound (1.0 equiv)	PPi		−7.92 (PPi)	−9.65 (PPi)	−4.83 (PPi)	−5.25 (PPi)	2.95 (HPO_4^{2-})
			−8.74 (ADP-β)	−8.93 (ATP-γ)	−6.51 (GDP-β)	−5.88 (GTP-γ)	−4.89 (PPi)
			−10.48 (ADP-α)	−10.77 (ATP-α)	−10.03 (GDP-α)	−10.44 (GTP-α)	
				−21.54 (ATP-β)		−20.77 (GTP−β)	
	ADP	−5.34 (PPi)		−9.73 (ADP-β)		−7.37 (ADP-β)	2.48 (HPO_4^{2-})
		−5.75 (ADP-β)		−10.65 (ADP-α)		−10.3 (ADP-α)	−6.38 (ADP-β)
		−10.3 (ADP-α)		−8.38 (ATP-γ)		−6.43 (GTP-γ)	−10.07 (ADP-α)
				−10.65 (ATP-α)		−10.48 (GTP-α)	
				−20.92 (ATP-β)		−20.51 (GTP-β)	
	ATP	−5.09 (PPi)	−9.31 (ADP-β)		−7.42 (GDP-β)		2.45 (HPO_4^{2-})
		−5.45 (ATP-γ)	−10.48 (ADP-α)		−10.06 (GDP-α)		−5.59 (ATP-γ)
		−10.62 (ATP-α)	−7.78 (ATP-γ)		−6.20 (ATP-γ)		−10.49 (ATP-α)
		−21.15 (ATP-β)	−10.69 (ATP-α)		−10.44 (ATP-α)		−20.15 (ATP-β)
			−20.48 (ATP-β)		−19.87 (ATP-β)		
	GDP	−5.28 (PPi)		−9.05 (GDP-β)		−7.01 (GDP-β)	2.64 (HPO_4^{2-})
		−5.74 (GDP-β)		−10.33 (GDP-α)		−10.25 (GDP-α)	−6.20 (GDP-β)
		−10.28 (GDP-α)		−7.43 (ATP-γ)		−6.24 (GTP-γ)	−10.13 (GDP-α)
				−10.55 (ATP-α)		−10.43 (GTP-α)	
				−20.28 (ATP-β)		−20.61 (GTP-β)	
	GTP	−5.21 (PPi)	−8.81 (ADP-β)		−6.81 (GDP-β)		2.73 (HPO_4^{2-})
		−5.512 (GTP-γ)	−10.33 (ADP-α)		−9.98 (GDP-α)		−5.45 (GTP-γ)
		−10.58 (GTP-α)	−6.75 (GTP-γ)		−5.69 (GTP-γ)		−10.45 (GTP-α)
		−20.14 (GTP-β)	−10.53 (GTP-α)		−10.34 (GTP-α)		−20.41 (GTP-β)
			−20.28 (GTP-β)		−19.90 (GTP-β)		
	HPO_4^{2-}	3.00 (HPO_4^{2-})	0.83 (HPO_4^{2-})	0.44 (HPO_4^{2-})	1.80 (HPO_4^{2-})	2.24 (HPO_4^{2-})	
		−5.40 (PPi)	−7.30 (ADP-β)	−7.75 (ATP-γ)	−6.55 (GDP-β)	−5.81 (GTP-γ)	
			−9.83 (ADP-α)	−10.63(ATP-α)	−9.78 (GDP-α)	−10.45 (GTP-α)	
				−20.62 (ATP-β)		−20.49 (GTP-β)	

titration in reverse order was also perfomed (see Figures S37−S44, Supporting Information). Titrations of ADP and ATP with **1**·PPi gave large chemical shift changes according to the PPi ^{31}P NMR spectroscopic peak up to δ −7.89 (ADP case) and −9.79 (ATP case) but not for GDP and GTP (PPi shows up at δ −5.33 and −5.50, respectively). To test for reversibility, an excess of **1** is titrated to the **1**:ADP:PPi mixture (1.0:1.0:5.0 equiv). This reveals that excess PPi binds with the added compound **1**, giving a downfield PPi signal shift, opposite to that found for titration of PPi to **1**·ADP (Figure S45, Supporting Information).

NMR spectroscopic studies also give some insights about PPi and Zn^{2+} binding (Figures S48−S50, Supporting Information). In the ^{31}P NMR spectrum in a HEPES H_2O buffer (pH 7.4) and D_2O mixture the **1**·PPi peak is positioned at δ −5.26 (free PPi δ −6.10). Then, addition of 3.0 equiv of Zn^{2+} to **1**·PPi gives a peak at δ −4.94. A downfield shift movement from δ −5.26 to δ −4.94 relates to the direction of the peak found for the PPi·Zn^{2+} complex (δ −5.18) not for that of free PPi. ^{1}H NMR spectral data reveal that there is in fact some minor decomposition and formation of salicylaldehyde upon addition of PPi and subsequent addition of Zn^{2+}. However, the level of fluorescence shows a possible reformation of the title compound. The aliphatic lysine portion becomes unclear and then resolved again. Since a generally higher concentration of species is required for NMR spectroscopic analysis, Zn^{2+} which is added as a dissolved species may be partially lost by way of coprecipitation; a very minor amount of unidentified white precipitate involving perhaps extra Cl^- present in compound **1**. In the ^{1}H NMR spectrum, addition of PPi is coincident with diminution of α- and β-carbonyl proton peaks (δ 3.86 and 1.81, respectively) (Figures S51−S53, Supporting Information); some traces of aldehyde are formed as well (δ 9.98, 7.45, 7.33, and 6.50). However, these peaks can be tentatively assigned to a salicylaldehyde PPi conjugate, not as the pure salicylaldehyde. Then, addition of excess Zn^{2+} (5.0 equiv) gives the return of the α- and β-carbonyl proton peaks and the pure salicylaldehyde peaks (δ 9.84, 7.67, 7.53, 7.03, and 6.93), suggesting incoming freshly added Zn^{2+} takes up PPi bound to compound **1** and possibly PPi that is conjugated with salicylaldehyde.

Tubulin Microtubule Formation and Fluorescence Study with Dinuclear Zinc(II) and Copper(II) Complexes. To address the practicality and novelty of this phosphate exchange behavior with dimetallic species (Scheme 1), an interface with a biological assay was used. Since tubulin involves GTP and GDP and has been made into a commercially available system (see Experimental Section), this convenient, but not inexpensive, assay was interfaced with the metal ion/phosphate manifold (Scheme 1). Here, changes in fluorescence intensity (λ_{exc} = 355 nm; $\lambda_{em,max}$ = 460 nm) helped elucidate stages of tubule growth in conjunction with paclitaxel (Pac), an activator of tubulin polymerization.[72] Paclitaxel was added into all samples and checked for differences of the extent of average microtubule polymerization (Figure 10). The greater the extent of microtubule growth, the higher the fluorescence intensity signal ($\lambda_{em,max}$ = 460 nm). GTP which binds into the growing microtubule is present at 1.0 mM in the assay. Separately, PPi and GDP were added at 1.0 mM as well. The dinuclear zinc(II) compound **1**, however, was too fluorescent at the observed

dx.doi.org/10.1021/ic201948c | Inorg. Chem. 2012, 51, 928−938

Table 5. ^{31}P NMR Spectroscopic Shift Results upon Gradual Titrations (0−5.0 equiv) to 1 and Bound Phosphates in D_2O Solvent

		titrant added gradually (0−5.0 equiv)				
		PPi	ADP	ATP	GDP	GTP
bound (1.0 equiv)	PPi			−4.64 → −9.79 (PPi)		−4.51 → −5.50 (PPi)
			−4.69 → −7.89 (PPi)	−5.53 → −9.26 (ATP-γ)	−4.50 → −5.33 (PPi)	−5.39 → −6.12 (GTP-γ)
			−6.12 → −8.83 (ADP-β)	−10.56 → −10.82 (ATP-α)	−6.09 → −7.02 (GDP-β)	−10.43 → −10.57 (GTP-α)
			−10.12 → −10.48 (ADP-α)	−20.24 → −21.83 (ATP-β)	−10.05 → −10.19 (GDP-α)	−20.29 → −20.88 (GTP-β)
	ADP			−5.94 → −9.90 (ADP-β)		−6.54 → −7.34 (ADP-β)
		−3.88 → −5.28 (PPi)		−9.10 → −10.64 (ADP-α)		−9.39 → −10.25 (ADP-α)
		−6.23 → −5.69 (ADP-β)		−5.40 → −8.69 (ATP-γ)		−5.36 → −6.59 (GTP-γ)
		−9.22 → −10.26 (ADP-α)		−10.48 → −10.69 (ATP-α)		−10.34 → −10.49 (GTP-α)
				−18.99 → −21.27 (ATP-β)		−19.35 → −21.70 (GTP-β)
	ATP		−5.42 → −7.47 (ATP-γ)		−5.48 → −6.33 (ATP-γ)	
		−4.15 → −5.28 (PPi)	−10.45 → −10.64 (ATP-α)		−10.50 → −10.46 (ATP-α)	
		−5.58 → −5.37 (ATP-γ)	−18.93 → −20.27 (ATP-β)		−19.02 → −19.88 (ATP-β)	
		−10.48 → −10.60 (ATP-α)	−6.72 → −9.15 (ADP-β)		−6.41 → −7.71 (GDP-β)	
		−18.99 → −21.15 (ATP-β)	−9.39 → −10.41 (ADP-α)		−9.40 → −10.16 (GDP-α)	
	GDP			−5.93 → −9.85 (GDP-β)		−6.59 → −7.34 (GDP-β)
		−3.91 → −5.27 (PPi)		−9.22 → −10.62 (GDP-α)		−9.46 → −10.29 (GDP-α)
		−6.17 → −5.73 (GDP-β)		−5.09 → −8.74 (ATP-γ)		−5.24 → −6.56 (GTP-γ)
		−9.31 → −10.27 (GDP-α)		−10.31 → −10.67 (ATP-α)		−10.30 → −10.49 (GTP-α)
				−18.76 → −21.15 (ATP-β)		−19.41 → −20.73 (GTP-β)
	GTP		−5.26 → −6.59 (GTP-γ)		−5.27 → −5.94 (GTP-γ)	
		−5.36 → −5.39 (GTP-γ)	−10.26 → −10.49 (GTP-α)		−10.26 → −10.38 (GTP-α)	
		−10.28 → −10.60 (GTP-α)	−19.56 → −20.14 (GTP-β)		−19.57 → −20.04 (GTP-β)	
		−19.57 → −21.18 (GTP-β)	−6.36 → −8.76 (ADP-β)		−6.28 → −7.34 (GDP-β)	
		−4.18 → −5.27 (PPi)	−9.65 → −10.31 (ADP-α)		−9.71 → −10.15 (GDP-α)	

dx.doi.org/10.1021/ic201948c | Inorg. Chem. 2012, 51, 928−938

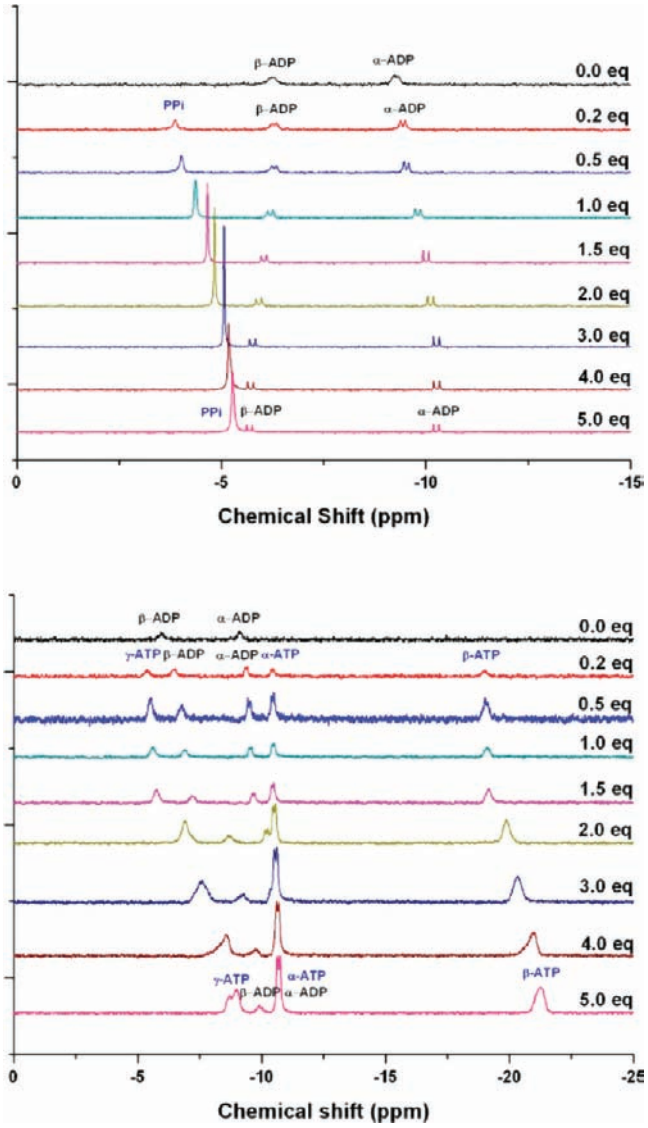

Figure 9. Stack plots of ^{31}P NMR spectra of (top) **1**·ADP with titration of PPi (0−5.0 equiv) and (bottom) **1**·ADP with titration of ATP (0−5.0 equiv) in D_2O.

wavelength; thus, a second set of trials with an analogous dinuclear copper(II) compound **2** was performed and interpreted (left). Here the F.I. results are more clear: PPi is thought to attach to **2** in the same way as it does to **1**. The nonfluorescent **2** showed ∼78% less intensity (inhibited the polymerization) than the control trial (Pac + tubulin) (Figure 10, bottom). Use of competing phosphates (PPi or GDP) with **2** has differing effects on growth inhibition: PPi showed higher intensity than for GDP. As PPi inhibits GTP binding at **2**, larger amounts of GTP are free for tubulin polymerization. For the array involving GDP showed the lowest intensity, less GDP is bound to **2**, more GTP is sequestered, and thus tubule growth is inhibited more than for PPi and **2** alone. Also, GDP inhibits tubule growth unlike PPi, which is more of a spectator when in the presence of tubulin and its dynamics. GDP/GTP interplay, in conjunction with a future optimized bimetallic complex, might interestingly inhibit or reverse tubulin polymerization. However, more experiments are needed to expand this new line of research and to approach the great complexities found naturally with tau-stabilized neuronal tubulin.

Scheme 1. Composite Diagram of Metal Ion Binding and Ligand Binding in which Optical Properties Are Modulated through Ligand Exchange of Compound 1[a]

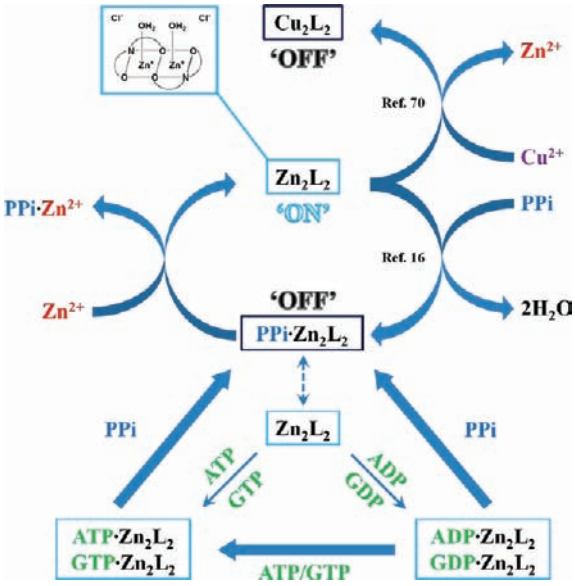

[a]ADP (sodium salt), ATP (disodium salt), GDP (sodium salt), GTP (sodium salt hydrate). Cu_2L_2 is the copper analogue of the dizinc species **1**.[70]

4. CONCLUSIONS

In this report, we discuss the displacement of diphosphate (ADP, GDP) by triphosphate (ATP, GTP) and PPi. Also, reversible fluorescence 'OFF−ON' behavior with sequential detection of PPi and Zn^{2+} was affected by the chiral dizinc Schiff-base complex **1** (Scheme 1). Operation of PPi and Zn^{2+} as inputs with the compound **1** substrate can be interpreted as implication (IMP) solution molecular logic gating. Direct displacement behavior with Cu^{2+} is effective in the presence of bound PPi. These trends are verified spectroscopically: ^{31}P NMR, UV−vis, emission, and CD spectroscopy. UV−vis spectra show the appearance of a new peak (∼392 nm); fluorescence quenching is detected with increasing amounts of titrant in all cases. Also, CD spectral studies in which signals disappeared helped confirm these trends. ^{31}P NMR spectroscopy yielded peak shifting toward the direction of the free phosphate in question for prebound species and in the direction of bound phosphates for the added titrant phosphate (at low equivalency). Such displacement was interfaced in biological cycle trials. α,β-Tubulin polymerization tubule assaying is controlled by processes involving GDP and GTP. A nonfluorescent copper complex (**2**), analogous to dizinc complex **1**, showed ∼78% less fluorescence intensity signifying a concomitant extent of polymerization inhibition. Use of PPi showed higher intensity than for GDP, indicating that the more GTP displaces and binds to the metallic dimer the more tubule growth is inhibited. This water-soluble fluorescent dizinc species can be useful as a new versatile Zn^{2+} molecular probe for research investigations related to neurodegenerative diseases and extensions to organophosphate detection remediation.[73]

■ ASSOCIATED CONTENT

Supporting Information

UV−vis, emission, and CD spectra of phosphate displacement and Zn^{2+} detection studies; various ^{1}H and ^{31}P NMR spectra

dx.doi.org/10.1021/ic201948c | Inorg. Chem. 2012, 51, 928−938

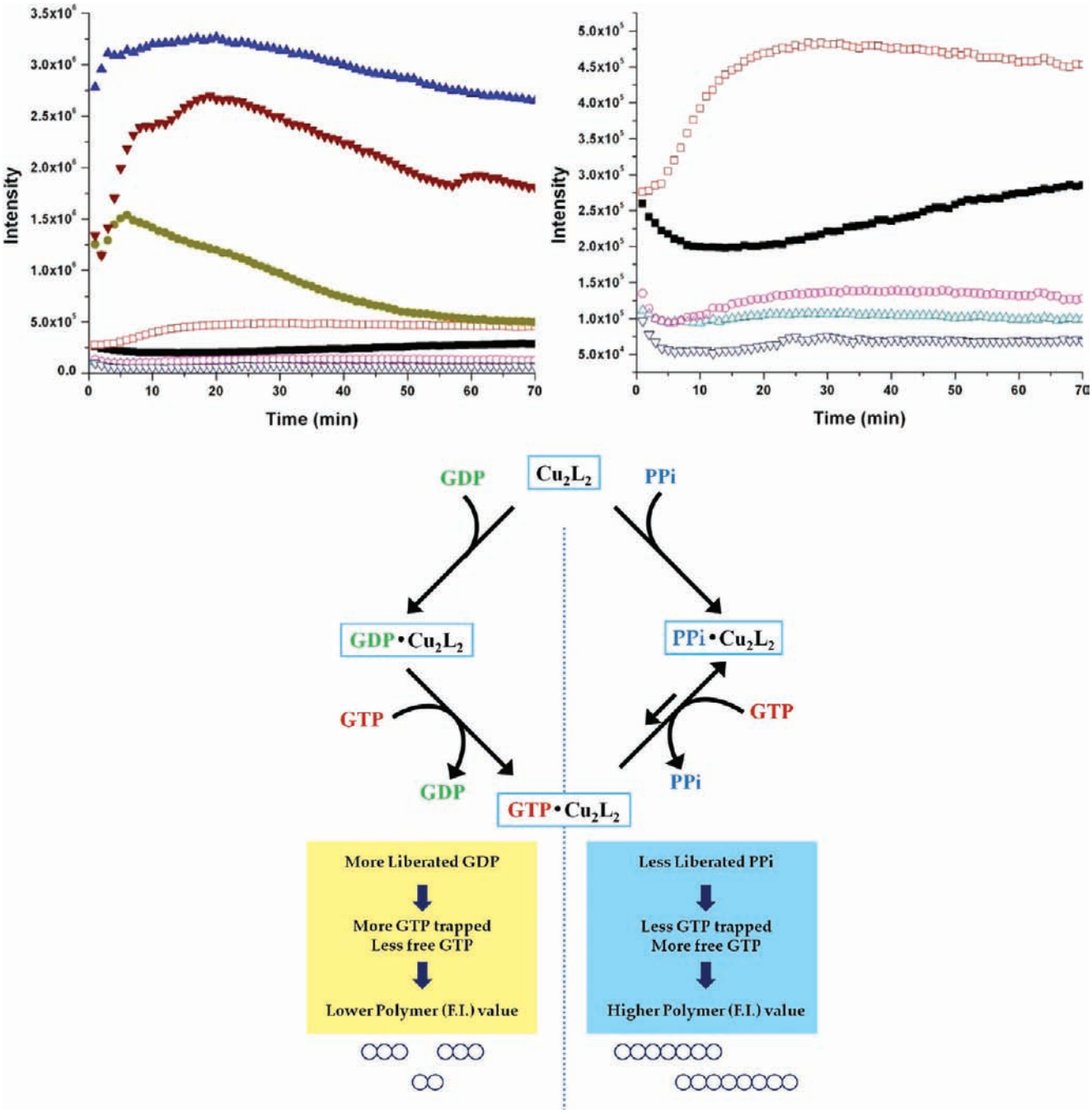

Figure 10. (Top left) Emission intensity change (λ_{exc} = 355 nm; $\lambda_{em,max}$ = 460 nm) depending on the tubulin polymerization assay by compounds **1** and **2**. (Top right) Magnification of the lower region of fluorescence intensity: (■) tubulin, (□) Pac + tubulin, (▲) Pac + tubulin + **1** (1.0 mM), (Δ) Pac + tubulin + **2** (1.0 mM), (●) Pac + tubulin + **1** (1.0 mM) + PPi (1.0 mM), (○) Pac + tubulin + **2** (1.0 mM) + PPi (1.0 mM), (▼) Pac + tubulin + **1** (1.0 mM) + GDP (1.0 mM), (▽) Pac + tubulin + **2** (1.0 mM) + GDP (1.0 mM). (Bottom) Scheme of proposed anion displacement and resulting tubulin polymerization.

and NMR titration graphs. This material is available free of charge via the Internet at http://pubs.acs.org.

■ AUTHOR INFORMATION

Corresponding Author

*E-mail: dchurchill@kaist.ac.kr.

■ ACKNOWLEDGMENTS

The Molecular Logic Gate Laboratory headed by DGC was supported financially for this work by the National Research Foundation of Korea (NRF), a grant funded by the Korea government (MEST) (nos. 2009-0070330 and 2010-0013660). Mr. Hack Soo Shin is gratefully acknowledged in enabling acquisition of ^{31}P NMR spectra. L.K. was an undergraduate Summer Intern in The Molecular Logic Gate Laboratory (April–June 2011) from Paris-Diderot University-Paris 7 (France).

■ REFERENCES

(1) Bowler, M. W.; Cliff, M. J.; Waltho, J. P.; Blackburn, G. M. *New J. Chem.* **2010**, *34*, 784.

(2) Hirsch, A. K. H.; Fischer, F. R.; Diederich, F. *Angew. Chem., Int. Ed.* **2007**, *46*, 338.
(3) Tabary, T.; Ju, L. Y.; Cohen, J. H. M. *J. Immunol. Methods* **1992**, *156*, 55.
(4) Nyren, P. *Anal. Biochem.* **1987**, *167*, 235.
(5) Kim, S. K.; Lee, D. H.; Hong, J. I.; Yoon, J. *Acc. Chem. Res.* **2009**, *42*, 23.
(6) Climent, E.; Casasus, R.; Marcos, M. D.; Martinez−Manez, R.; Sancenon, F.; Soto, J. *Dalton Trans.* **2009**, 4806.
(7) Chen, K. H.; Liao, J. H.; Chan, H. Y.; Fang, J. M. *J. Org. Chem.* **2009**, *74*, 895.
(8) Wang, H.; Chan, W. H. *Org. Biomol. Chem.* **2008**, *6*, 162.
(9) Climent, E.; Casasus, R.; Marcos, M. D.; Martinez−Manez, R.; Sancenon, F.; Soto, J. *Chem. Commun.* **2008**, 6531.
(10) Swamy, K. M. K.; Kwon, S. K.; Lee, H. N.; Kumar, S. M. S.; Kim, J. S.; Yoon, J. *Tetrahedron Lett.* **2007**, *48*, 8683.
(11) Singh, N. J.; Jun, E. J.; Chellappan, K.; Thangadurai, D.; Chandran, R. P.; Hwang, I. C.; Yoon, J.; Kim, K. S. *Org. Lett.* **2007**, *9*, 485.
(12) Ojida, A.; Miyahara, Y.; Wongkongkatep, A.; Tamaru, S.; Sada, K.; Hamachi, I. *Chem. Asian J.* **2006**, *1*, 555.
(13) Liao, J. H.; Chen, C. T.; Fang, J. M. *J. Chin. Chem. Soc.* **2006**, *53*, 1439.
(14) Marcotte, N.; Taglietti, A. *Supramol. Chem.* **2003**, *15*, 617.
(15) Aldakov, D.; Anzenbacher, P. *Chem. Commun.* **2003**, 1394.
(16) Khatua, S.; Choi, S. H.; Lee, J.; Kim, K.; Do, Y.; Churchill, D. G. *Inorg. Chem.* **2009**, *48*, 2993.
(17) Ambrosi, G.; Formica, M.; Fusi, V.; Giorgi, L.; Guerri, A.; Macedi, E.; Micheloni, M.; Paoli, P.; Pontellini, R.; Rossi, P. *Inorg. Chem.* **2009**, *48*, 5901.
(18) Lee, J. H.; Park, J.; Lah, M. S.; Chin, A.; Hong, J. I. *Org. Lett.* **2007**, *9*, 3729.
(19) Lee, H. N.; Swamy, K. M. K.; Kim, S. K.; Kwon, J. Y.; Kim, Y.; Kim, S. J.; Yoon, Y. J.; Yoon, J. *Org. Lett.* **2007**, *9*, 243.
(20) Jang, Y. J.; Jun, E. J.; Lee, Y. J.; Kim, Y. S.; Kim, J. S.; Yoon, J. *J. Org. Chem.* **2005**, *70*, 9603.
(21) Lee, D. H.; Kim, S. Y.; Hong, J. I. *Angew. Chem., Int. Ed.* **2004**, *43*, 4777.
(22) Ravikumar, I.; Ghosh, P. *Inorg. Chem.* **2011**, *50*, 4229.
(23) Comes, M.; Marcos, M. D.; Martinez−Manez, R.; Sancenon, F.; Soto, J.; Villaescusa, L. A.; Amoros, P. *Chem. Commun.* **2008**, 3639.
(24) Hanshaw, R. G.; Hilkert, S. M.; Hua, J.; Smith, B. D. *Tetrahedron Lett.* **2004**, *45*, 8721.
(25) Buratta, M.; Piccotti, L.; Giannini, S.; Gresele, P.; Roberti, R.; Corazzi, L. *J. Membr. Biol.* **2006**, *212*, 199.
(26) Zhang, B. L.; Zhang, Y. Q.; Shacter, E.; Zheng, Y. *Biochemistry* **2005**, *44*, 2566.
(27) Wittinghofer, F. *Nature* **1998**, *394*, 317.
(28) Grover, S.; Hamel, E. *Eur. J. Biochem.* **1994**, *222*, 163.
(29) Frieden, C.; Patane, K. *Biochemistry* **1988**, *27*, 3812.
(30) Kim, K.; Churchill, D. G. In *Radionuclides in the Environment*, 1st ed.; Atwood, D. A., Ed.; Wiley: New York, 2010; p 109.
(31) Haas, K. L.; Franz, K. J. *Chem. Rev.* **2009**, *109*, 4921.
(32) Eide, D. J. *Annu. Rev. Nutr.* **1998**, *18*, 441.
(33) Holm, R. H.; Kennepohl, P.; Solomon, E. I. *Chem. Rev.* **1996**, *96*, 2239.
(34) Zatta, P.; Drago, D.; Bolognin, S.; Sensi, S. L. *Trends Pharmacol. Sci.* **2009**, *30*, 346.
(35) Drago, D.; Bolognin, S.; Zatta, P. *Curr. Alzheimer Res.* **2008**, *5*, 500.
(36) Que, E. L.; Domaille, D. W.; Chang, C. J. *Chem. Rev.* **2008**, *108*, 1517.
(37) Dineley, K. E.; Votyakova, T. V.; Reynolds, I. J. *J. Neurochem.* **2003**, *85*, 563.
(38) Takeda, A. *Biometals* **2001**, *14*, 343.
(39) Nolan, E. M.; Lippard, S. J. *Acc. Chem. Res.* **2009**, *42*, 193.
(40) Domaille, D. W.; Que, E. L.; Chang, C. J. *Nat. Chem. Biol.* **2008**, *4*, 168.
(41) Zhou, X. B.; Lu, Y. G.; Zhu, J. F.; Chan, W. H.; Lee, A. W. M.; Chan, P. S.; Wong, R. N. S.; Mak, N. K. *Tetrahedron* **2011**, *67*, 3412.
(42) Xu, Z. C.; Kim, G. H.; Han, S. J.; Jou, M. J.; Lee, C.; Shin, I.; Yoon, J. *Tetrahedron* **2009**, *65*, 2307.
(43) Huang, S.; Clark, R. J.; Zhu, L. *Org. Lett.* **2007**, *9*, 4999.
(44) Yang, R. H.; Li, K. A.; Wang, K. M.; Zhao, F. L.; Li, N.; Liu, F. *Anal. Chem.* **2003**, *75*, 612.
(45) Hanaoka, K.; Kikuchi, K.; Kojima, H.; Urano, Y.; Nagano, T. *Angew. Chem., Int. Ed.* **2003**, *42*, 2996.
(46) de Silva, A. P. *Chem. Asian J.* **2011**, *6*, 750.
(47) de Silva, A. P.; Uchiyama, S. *Nat. Nanotechnol.* **2007**, *2*, 399.
(48) de Silva, A. P.; Gunaratne, H. Q. N.; Gunnlaugsson, T.; Huxley, A. J. M.; McCoy, C. P.; Rademacher, J. T.; Rice, T. E. *Chem. Rev.* **1997**, *97*, 1515.
(49) de Silva, A. P.; Gunaratne, H. Q. N.; McCoy, C. P. *Nature* **1993**, *364*, 42.
(50) Straight, S. D.; Andreasson, J.; Kodis, G.; Bandyopadhyay, S.; Mitchell, R. H.; Moore, T. A.; Moore, A. L.; Gust, D. *J. Am. Chem. Soc.* **2005**, *127*, 9403.
(51) Uchiyama, S.; Kawai, N.; de Silva, A. P.; Iwai, K. *J. Am. Chem. Soc.* **2004**, *126*, 3032.
(52) Guo, X. F.; Zhang, D. Q.; Zhu, D. B. *Adv. Mater.* **2004**, *16*, 125.
(53) Callan, J. F.; de Silva, A. P.; McClenaghan, N. D. *Chem. Commun.* **2004**, 2048.
(54) Ami, S.; Hliwa, M.; Joachim, C. *Chem. Phys. Lett.* **2003**, *367*, 662.
(55) Wang, S. C.; Men, G. W.; Zhao, L. Y.; Hou, Q. F.; Jiang, S. M. *Sens. Actuators, B* **2010**, *145*, 826.
(56) Upadhyay, K. K.; Kumar, A.; Mishra, R. K.; Fyles, T. M.; Upadhyay, S.; Thapliyal, K. *New J. Chem.* **2010**, *34*, 1862.
(57) Strack, G.; Ornatska, M.; Pita, M.; Katz, E. *J. Am. Chem. Soc.* **2008**, *130*, 4234.
(58) Rurack, K.; Trieflinger, C.; Koval'chuck, A.; Daub, J. *Chem.—Eur. J.* **2007**, *13*, 8998.
(59) Sarkar, M.; Banthia, S.; Patil, A.; Ansari, M. B.; Samanta, A. *New J. Chem.* **2006**, *30*, 1557.
(60) de Silva, A. P.; McClenaghan, N. D. *Chem.—Eur. J.* **2002**, *8*, 4935.
(61) Bonne, D.; Heusele, C.; Simon, C.; Pantaloni, D. *J. Biol. Chem.* **1985**, *260*, 2819.
(62) Nogales, E.; Wolf, S. G.; Downing, K. H. *Nature* **1998**, *391*, 199.
(63) Desai, A.; Mitchison, T. J. *Annu. Rev. Cell Dev. Biol.* **1997**, *13*, 83.
(64) Jackson, J. R.; Patrick, D. R.; Dar, M. M.; Huang, P. S. *Nat. Rev. Cancer* **2007**, *7*, 107.
(65) Lichtenberg, B.; Mandelkow, E. M.; Hagestedt, T.; Mandelkow, E. *Nature* **1988**, *334*, 359.
(66) Bramblett, G. T.; Goedert, M.; Jakes, R.; Merrick, S. E.; Trojanowski, J. Q.; Lee, V. M. Y. *Neuron* **1993**, *10*, 1089.
(67) Bulic, B.; Pickhardt, M.; Schmidt, B.; Mandelkow, E. M.; Waldmann, H.; Mandelkow, E. *Angew. Chem., Int. Ed.* **2009**, *48*, 1741.
(68) Khatua, S.; Kim, K.; Kang, J.; Huh, J. O.; Hong, C. S.; Churchill, D. G. *Eur. J. Inorg. Chem.* **2009**, 3266.
(69) Valeur, B.; Pouget, J.; Bourson, J.; Kaschke, M.; Ernsting, N. P. *J. Phys. Chem.* **1992**, *96*, 6545.
(70) Khatua, S.; Choi, S. H.; Lee, J.; Huh, J. O.; Do, Y.; Churchill, D. G. *Inorg. Chem.* **2009**, *48*, 1799.
(71) Hancock, C. R.; Brault, J. J.; Wiseman, R. W.; Terjung, R. L.; Meyer, R. A. *Am. J. Physiol.−Cell Physiol.* **2005**, *288*, C1298.
(72) Dabydeen, D. A.; Florence, G. J.; Paterson, I.; Hamel, E. *Cancer Chemother. Pharmacol.* **2004**, *53*, 397.
(73) Kim, K.; Tsay, O. G.; Atwood, D. A.; Churchill, D. G. *Chem. Rev.* **2011**, *111*, 5345.